

Generalized $ABCD$ propagation for interacting atomic clouds.

F. Impens^{1,2} and Ch. J. Bordé^{1,3}

¹ *SYRTE, Observatoire de Paris, CNRS, 61 avenue de l'Observatoire, 75014 Paris, France*

² *Instituto de Física, Universidade Federal do Rio de Janeiro. Caixa Postal 68528, 21941-972 Rio de Janeiro, RJ, Brasil and*

³ *Laboratoire de Physique des Lasers, Institut Galilée, F-93430 Villetaneuse, France*

(Dated: February 6, 2020)

We present a treatment of the nonlinear matter wave propagation inspired from optical methods, which includes interaction effects within the atom optics equivalent of the aberrationless approximation. The atom-optical ABCD matrix formalism, considered so far for non-interacting clouds, is extended perturbatively beyond the linear regime of propagation. This approach, applied to discuss the stability of a matter-wave resonator involving a free-falling sample, agrees very well with the predictions of the full nonlinear paraxial wave equation. An alternative optical treatment of interaction effects, based on the aberrationless approximation and suitable for cylindrical paraxial beams of uniform linear density, is also adapted for matter waves.

PACS numbers: 03.75.Pp, 03.75.-b, 42.65.Jx, 41.85.Ew, 31.15-Md

I. INTRODUCTION

Light and matter fields are governed by similar equations of motion [1]. Both photons and atoms interact in a symmetrical manner: atom-atom interactions are mediated through photons, while photon-photon interactions are mediated through atoms. Before the advent of Bose-Einstein condensation, two groups realized independently that atomic dipole-dipole interactions give rise to a cubic nonlinearity in the propagation equation analogous to that induced by the Kerr effect [2, 3]. Following this analogy, the field of non-linear atom optics emerged in the last decade, leading to the experimental verification with matter waves of several well-known nonlinear optical phenomena: the four-wave mixing [4], the formation of solitons [5, 6, 7, 8] and of vortices [9, 10], the superradiance [11] and the coherent amplification [12]. The nonlinear propagation of matter waves has been the object of extensive experimental [13, 14] and theoretical work, among which the time-dependent Thomas-Fermi approximation [15], the variational approach [16], and more recently the method of moments [17]. These treatments have been used successfully to obtain analytical expressions in good agreement with the exact solution of the 3D nonlinear Schrödinger equation (NLSE).

There exists, for cylindrical wave-packets propagating in the paraxial regime, a very elegant method to handle this equation which has been used in optics to treat self-focusing effects [18, 19]. It relies on the “aberrationless approximation”, assuming that the nonlinearity is sufficiently weak as to preserve the shape of a fundamental Gaussian mode, and it involves a generalized complex radius of curvature. This treatment is equally relevant for the paraxial propagation of cylindrical matter waves, and it is presented in this context in Appendix A. Unfortunately, the assumptions required - such as the constant longitudinal velocity and the paraxial propagation - limit the scope of this approach, which appears as too stringent to describe the matter wave propagation in most experiments.

This motivates the introduction of a different analytical method to obtain approximate solutions for the NLSE in a more general propagation regime. This is the central contribution of this paper, which exposes a perturbative matrix analysis especially well-suited to discuss the stability of a matter-wave resonator. With an Hamiltonian quadratic in position and momentum operators, and in the absence of atomic interactions, the Schrödinger equation admits a basis of Gaussian solutions. Their evolution is easily obtained through a time-dependent matrix denoted “ABCD” [1, 20], in analogy with the propagation of optical rays in optics [21]. In the “aberrationless approximation”, it is possible to extend this treatment to include perturbatively interaction effects and obtain the propagation of a fundamental Gaussian mode with a modified “ABCD” matrix. As an illustration of this method, the stability of a matter-wave resonator is analyzed thanks to this “ABCD” matrix, which encapsulates the divergence resulting from the mean-field potential. An ABCD-matrix approach had already been used in [13] to characterize the divergence of a weakly outcoupled atom laser beam due to interactions with the source condensate. The present treatment is sensibly different, since it is not restricted to the paraxial regime and since it addresses rather self-interaction effects in the beam propagation.

Our approach is indeed mainly inspired from previous theoretical developments in optics, which aimed at treating the wave propagation in a Kerr medium through such a matrix formalism [18]. An approach of the non-linearity based on the resulting frequency-dependent diffraction [22] successfully explained the asymmetric profile of atomic

and molecular intra-cavity resonances [23], as well as the dynamics of Gaussian modes in ring and two-isotopes lasers [24, 25]. Later, a second-order polynomial determined by a least-square fit of the wave intensity profile was considered to model the Kerr effect [26]. In this paper, we explore the quantum mechanical counterpart of this strategy: mean-field interactions are modelled thanks to a second-order polynomial, determined perturbatively from the wave-function, and which can be interpreted in optical terms.

II. LENSING POTENTIAL

One considers the propagation of a zero-temperature condensate in a uniform gravity field and in the mean-field approximation. The corresponding Hamiltonian reads:

$$\hat{H} = \frac{\hat{\mathbf{p}}^2}{2m} + mgz + g_i |\phi(\hat{\mathbf{r}}, t)|^2 \quad (1)$$

g_i is the coupling constant related to the diffusion length a and to the number of atoms N by $g_i = 4\pi N \hbar^2 a / m$. Our purpose is to approximate the mean-field potential $g_i |\phi(\mathbf{r}, t)|^2$ by an operator leading to an easily solvable wave equation and as close as possible to the interaction potential. A second-order polynomial in the position and momentum operators is a suitable choice, since it allows to obtain Gaussian solutions to the propagation equation. We note $\hat{H}_0 = \frac{\hat{\mathbf{p}}^2}{2m} + mgz$ the interaction-free Hamiltonian and

$$\hat{H}(\hat{\mathbf{r}}, \hat{\mathbf{p}}, t) = \hat{H}_0 + P_l(\hat{\mathbf{r}}, \hat{\mathbf{p}}, t) \quad (2)$$

the quadratic Hamiltonian accounting for interactions effects.

The strategy exposed in this paper consists in picking up, among the possible polynomials P , the element which minimizes an appropriate distance measure to the mean-field potential. In geometric terms, this polynomial appears as the projection of the mean-field potential onto the vector space spanned by second-order polynomials in position and momentum. This potential will be referred to as the ‘‘lensing potential’’, denomination which will be justified in Sec. IV. We define a distance analogous to the error function used in [26], which involves the polynomial P and the quantum state $|\phi(t)\rangle$ resulting from the non-linear evolution:

$$E(P(t), |\phi(t)\rangle) = \int d^3\mathbf{r} |\langle \mathbf{r} | P(\hat{\mathbf{r}}, \hat{\mathbf{p}}, t) |\phi(t)\rangle - g_i |\phi(\mathbf{r}, t)|^2 \phi(\mathbf{r}, t) |^2 \quad (3)$$

The minimization of the distance $E(P(t), |\phi(t)\rangle)$ for the lensing potential $P_l(t)$ implies that the function E is stationary towards any second-order polynomial coefficient at the point $(P_l(t), |\phi(t)\rangle)$:

$$\forall t \geq t_0 \quad \nabla_P E(P_l(t), |\phi(t)\rangle) = 0 \quad (4)$$

We have noted ∇_P the gradient associated with the coefficients of a second-order polynomial, and t_0 is the initial time from which we compute the evolution of the wave-function - we assume that $\phi(\mathbf{r}, t_0)$ is known -. The determination of the lensing potential associated with self-interactions in the beam indeed requires previous knowledge of the wave-function evolution. This difficulty did not arise in other optical treatments of atomic interaction effects [13, 27, 28], in which the atomic beam propagation was mainly affected by interactions with a different sample of well-known wave-function. This is typically the case for a weakly outcoupled continuous atom laser beam, in which the diverging lens effect results from the source condensate. We propose to circumvent this self-determination problem thanks to a perturbative treatment. Such approach is legitimate for the diluted matter waves involved in usual atom interferometers. The first-order lensing polynomial and the corresponding Hamiltonian $\hat{H}^{(1)}(t) = \hat{H}_0 + P_l^{(1)}(\hat{\mathbf{r}}, \hat{\mathbf{p}}, t)$ are determined from the linear evolution, according to:

$$\forall t \geq t_0 \quad \nabla_P E\left(P_l^{(1)}(t), e^{-i/\hbar \hat{H}_0(t-t_0)} |\phi(t_0)\rangle\right) = 0 \quad (5)$$

Higher-order lensing effects can be computed iteratively. For instance, the second-order lensing polynomial $P_l^{(2)}(t)$ satisfies:

$$\forall t \geq t_0 \quad \nabla_P E\left(P_l^{(2)}(t), T\left[e^{-i/\hbar \int_{t_0}^t dt' [\hat{H}_0 + P_l^{(1)}(\hat{\mathbf{r}}, \hat{\mathbf{p}}, t')]} |\phi(t_0)\rangle\right]\right) = 0$$

where we have used the usual time-ordering operator T [29].

III. OPTICAL PROPAGATION OF MATTER WAVES: THE ABCD THEOREM.

This section gives a remainder on a general result - called the *ABCD* theorem - concerning the propagation of matter waves in a time-dependent quadratic potential, which is the atomic counterpart of the ray matrix formalism frequently used in optics [21]. It shows that the evolution of a Gaussian wave-function under an Hamiltonian quadratic in position and momentum is similar to the propagation of a Gaussian mode of the electric field in a linear optical system. A detailed description of this theoretical result of atom optics is given in the references [20, 30].

One considers a time-dependent quadratic Hamiltonian such as:

$$H(\hat{\mathbf{r}}, \hat{\mathbf{p}}, t) = \frac{\hat{\tilde{\mathbf{p}}}\beta(t)\hat{\tilde{\mathbf{p}}}}{2m} + \frac{1}{2}\hat{\tilde{\mathbf{p}}}\alpha(t)\hat{\mathbf{r}} - \frac{1}{2}\hat{\mathbf{r}}\delta(t)\hat{\tilde{\mathbf{p}}} - \frac{m}{2}\hat{\mathbf{r}}\gamma(t)\hat{\mathbf{r}} - m\mathbf{g}(t) \cdot \hat{\mathbf{r}} + \mathbf{f}(t) \cdot \hat{\mathbf{p}} + h(t) \quad (6)$$

$\alpha(t)$, $\beta(t)$, $\gamma(t)$ and $\delta(t)$ are 3×3 matrices [i]; $\mathbf{f}(t)$ and $\mathbf{g}(t)$ are three-dimensional vectors; $h(t)$ is a scalar, and $\tilde{}$ stands for the transposition. Such Hamiltonian is appropriate to describe many physical effects [ii] as detailed in [31], and we use it here simply to approximate the nonlinear Hamiltonian (1).

A. *ABCD* propagation of a Gaussian wave-function.

The propagation of a Gaussian wave-packet in such an Hamiltonian can be described simply as follows. Let $\phi(\mathbf{r}, t)$ be an atomic wave packet initially given by:

$$\phi(\mathbf{r}, t_0) = \frac{1}{\sqrt{|\det X_0|}} \exp \left[\frac{im}{2\hbar} (\mathbf{r} - \mathbf{r}_{c0}) Y_0 X_0^{-1} (\mathbf{r} - \mathbf{r}_{c0}) + \frac{i}{\hbar} \mathbf{p}_{c0} \cdot (\mathbf{r} - \mathbf{r}_{c0}) \right] \quad (7)$$

The 3×3 complex matrices X_0 , Y_0 represent the initial width of the wave packet in position and momentum respectively: $X_0 = iD(\Delta x(t_0), \Delta y(t_0), \Delta z(t_0))$ and $Y_0 = D(\Delta p_x(t_0), \Delta p_y(t_0), \Delta p_z(t_0))$, with D standing for a diagonal matrix. The vectors \mathbf{r}_{c0} , \mathbf{p}_{c0} give the initial average position and momentum. The *ABCD* theorem for matter waves states that, at any time $t \geq t_0$, the wave-packet $\phi(\mathbf{r}, t)$ satisfies:

$$\phi(\mathbf{r}, t) = \frac{e^{\frac{i}{\hbar} S(t, t_0, \mathbf{r}_{c0}, \mathbf{p}_{c0})}}{\sqrt{|\det X(t)|}} \exp \left[\frac{im}{2\hbar} (\mathbf{r} - \mathbf{r}_c(t)) Y(t) X^{-1}(t) (\mathbf{r} - \mathbf{r}_c(t)) + \frac{i}{\hbar} \mathbf{p}_{c0}(t) \cdot (\mathbf{r} - \mathbf{r}_c(t)) \right]$$

$S(t, t_0, \mathbf{r}_{c0}, \mathbf{p}_{c0})$ is the classical action evaluated between t and t_0 of a point-like particle which motion follows the classical Hamiltonian $H(\mathbf{r}, \mathbf{p}, t)$ and with respective initial position and momentum $\mathbf{r}_{c0}, \mathbf{p}_{c0}$. The width matrices in position $X(t)$ and momentum $Y(t)$, and the average position and momentum $\mathbf{r}_c(t), \mathbf{p}_c(t)$ are determined through the same 6×6 “*ABCD*” matrix:

$$\begin{aligned} \begin{pmatrix} \mathbf{r}_c(t) \\ \frac{1}{m} \mathbf{p}_c(t) \end{pmatrix} &= \begin{pmatrix} A(t, t_0) & B(t, t_0) \\ C(t, t_0) & D(t, t_0) \end{pmatrix} \begin{pmatrix} \mathbf{r}_{c0} \\ \frac{1}{m} \mathbf{p}_{c0} \end{pmatrix} + \begin{pmatrix} \xi(t, t_0) \\ \phi(t, t_0) \end{pmatrix} \\ \begin{pmatrix} X(t) \\ Y(t) \end{pmatrix} &= \begin{pmatrix} A(t, t_0) & B(t, t_0) \\ C(t, t_0) & D(t, t_0) \end{pmatrix} \begin{pmatrix} X_0 \\ Y_0 \end{pmatrix} \end{aligned}$$

The *ABCD* matrix and the vectors ξ, ϕ can be expressed formally as [32]:

$$M(t, t_0) = \begin{pmatrix} A(t, t_0) & B(t, t_0) \\ C(t, t_0) & D(t, t_0) \end{pmatrix} = T \left[\exp \left(\int_{t_0}^t dt' \begin{pmatrix} \alpha(t') & \beta(t') \\ \gamma(t') & \delta(t') \end{pmatrix} \right) \right] \quad (8)$$

$$\begin{pmatrix} \xi(t, t_0) \\ \phi(t, t_0) \end{pmatrix} = \int_{t_0}^t dt' M(t, t') \begin{pmatrix} \mathbf{f}(t') \\ \mathbf{g}(t') \end{pmatrix} \quad (9)$$

Although the former expressions seem rather involved, in all cases of practical interest, the *ABCD* $\xi\phi$ parameters can be determined analytically or at least by efficient numerical methods.

[i] $\delta(t) = -\tilde{\alpha}(t)$ to ensure the Hamiltonian hermiticity

[ii] To mention a few, the quadratic term with $\gamma(t)$ models a gravity gradient, the tensor $\alpha(t)$ can account for the Sagnac or Lense-Thirring effects, and the tensor $\beta(t)$ for gravitational waves.

B. Physical interpretation of the $ABCD$ propagation.

The phase-space propagation provides a relevant insight in the transformation operated by the $ABCD$ matrix. Consider the Wigner distribution of a single-particle density operator evolving under the Hamiltonian (6). The Wigner distribution at time t is related to the distribution at time t_0 by the following map:

$$W(\mathbf{r}, \mathbf{p}, t) = W\left(\tilde{D}(\mathbf{r} - \xi) - \frac{1}{m}\tilde{B}(\mathbf{p} - m\phi), -m\tilde{C}(\mathbf{r} - \xi) + \tilde{A}(\mathbf{p} - m\phi), t_0\right)$$

where the matrices A, B, C, D and vectors ξ, ϕ are again evaluated at the couple of instants (t, t_0) . The action of the evolution operator onto the Wigner distribution is thus amenable to a time-dependent linear map. The fact that $ABCD$ matrices are symplectic [20] implies that this map is unitary: such evolution preserves the global phase-space volume, and the quality factor of an atomic beam in the sense of [33].

The Gross Pitaevskii Equation actually does not lead to a motion which preserves the phase-space density: for instance, repulsive interactions increase the divergence of an atom laser beam [13, 27]. We choose nonetheless to approximate the non-linear evolution with a phase-space preserving map, determined here through a quadratic approximation of the Hamiltonian. This is the atom-optical aberrationless approximation, which proceeds as in optics, where the light beam propagation in a Kerr medium is described without considering the generation of higher-order modes, i.e. with a constant beam quality factor and phase-space density.

IV. ABCD MATRIX A FREE-FALLING INTERACTING ATOMIC CLOUD.

Let us apply the method discussed above to describe the propagation of a free-falling Gaussian atomic wave-packet. In the aberrationless approximation, such a wave-packet is simply determined by the parameters $ABCD\xi\phi$ and by the phase associated with the action. In view of the resonator stability analysis, we will focus on the computation of the $ABCD$ matrix in presence of the mean-field potential. We consider only the leading-order nonlinear corrections, associated with the first-order lensing polynomial $P_l^{(1)}(\mathbf{r}, \mathbf{p}, t)$.

This section begins with the determination of this potential defined by Eq. (5). A formal expression of the atom-optical $ABCD$ matrix, taking into account this lensing potential, is obtained. An infinitesimal expansion of this expression shows that the mean-field interactions effectively play the role of a divergent lens: the atom-optical $ABCD$ matrix of the free-falling cloud evolution is similar to the optical $ABCD$ matrix associated with the propagation of a light ray through a series of infinitesimal divergent lenses. In our case, the propagation axis is the time, and the infinitesimal lenses correspond to the action of the mean-field potential in infinitesimal time slices.

A. Determination of the lensing potential.

We assume that the condensate, evolving in the Hamiltonian (1), is initially at rest and described by a Gaussian wavefunction:

$$\phi(x, y, z, t_0) = \frac{\pi^{-3/4}}{\sqrt{w_x(t_0)w_y(t_0)w_z(t_0)}} e^{-\frac{x^2}{2w_x(t_0)^2} - \frac{y^2}{2w_y(t_0)^2} - \frac{z^2}{2w_z(t_0)^2}}$$

It is easy to show that, when one considers the interaction-free evolution, the widths are given at time $t \geq t_0$ by:

$$w_i(t) = \sqrt{w_i^2(t_0) + \frac{\hbar^2}{m^2 w_i^2(t_0)}(t - t_0)^2}$$

This result can be easily retrieved by considering the initial width matrices $X_0 = iD(w_x(t_0), w_y(t_0), w_z(t_0))$ and $Y_0 = \frac{\hbar}{m}D(1/w_x(t_0), 1/w_y(t_0), 1/w_z(t_0))$ for the wave-function, and applying the free $ABCD$ matrix [20]:

$$\begin{pmatrix} A(t, t_0) & B(t, t_0) \\ C(t, t_0) & D(t, t_0) \end{pmatrix} = \begin{pmatrix} 1 & t - t_0 \\ 0 & 1 \end{pmatrix} \quad (10)$$

The square of the free-evolving wave-function thus reads:

$$|\phi^{(0)}(\mathbf{r}, t)|^2 = \frac{\pi^{-3/2}}{w_x(t)w_y(t)w_z(t)} \exp \left[-\frac{(x - x_c(t))^2}{w_x(t)^2} - \frac{(y - y_c(t))^2}{w_y(t)^2} - \frac{(z - z_c(t))^2}{w_z(t)^2} \right]$$

We use this expression to determine the first-order lensing polynomial $P_l^{(1)}(\mathbf{r}, \mathbf{p}, t)$. Since this operator acts on Gaussian wave-functions, differentiation is equivalent to the multiplication by a position coordinate, so the action of the momentum operator is indeed equivalent to that of the position operator up to a multiplicative constant. One can thus, without any loss of generality, search for a lensing polynomial $P_l^{(1)}(\mathbf{r}, t)$ involving only the position operator, and minimizing the following error function:

$$E(P(t), |\phi^{(0)}(t)\rangle) = \int d^3\mathbf{r} |\phi^{(0)}(\mathbf{r}, t)|^2 \left(P(\mathbf{r}, t) - g_i |\phi^{(0)}(\mathbf{r}, t)|^2 \right)^2$$

Expanding the polynomial $P_l^{(1)}(\mathbf{r}, t)$ around the central position $\mathbf{r}_c(t)$, a parity argument shows that the linear terms vanish:

$$P_l^{(1)}(\mathbf{r}, t) = g_i [c_0(t) - c_x(t)(x - x_c(t))^2 - c_y(t)(y - y_c(t))^2 - c_z(t)(z - z_c(t))^2]$$

By definition of the lensing polynomial, the error function (11) must be stationary with respect to each coefficient $c_{x,y,z,0}(t)$, which leads to:

$$c_0(t) = \frac{7}{4V(t)} \quad c_{x,y,z}(t) = \frac{1}{2w_{x,y,z}(t)^2 V(t)} \quad V(t) = (2\pi)^{3/2} \prod_{i=x,y,z} w_i(t) \quad (11)$$

Only the quadratic term intervene in the $ABCD$ matrix: the coefficient $c_0(t)$ merely adds a global additional phase to the wave-function, which does not change the subsequent stability analysis.

B. Formal expression of the effective $ABCD$ matrix.

We can readily express the $ABCD$ matrix associated with the evolution under $\hat{H}^{(1)}(t)$. Writing this Hamiltonian in the form of Eq. (6), and using the formal expression (8) of the $ABCD$ matrix as a time-ordered series, one obtains:

$$M^{(1)}(t, t_0, X_0) = \begin{pmatrix} A^{(1)}(t, t_0, X_0) & B^{(1)}(t, t_0, X_0) \\ C^{(1)}(t, t_0, X_0) & D^{(1)}(t, t_0, X_0) \end{pmatrix} = T \left[\exp \left(\int_{t_0}^t dt' \begin{pmatrix} \alpha^{(1)}(t') & \beta^{(1)}(t') \\ \gamma^{(1)}(t') & \delta^{(1)}(t') \end{pmatrix} \right) \right] \quad (12)$$

In contrast to the usual linear $ABCD$ matrices, this matrix now depends on the input vector through the initial position width matrix X_0 [i]. A brief inspection of Eq. (6) and of the Hamiltonian $\hat{H}^{(1)}(t)$

$$\hat{H}^{(1)}(t) = \frac{\hat{\mathbf{p}}^2}{2m} + mgz + g_i [c_0(t) - c_x(t)(x - x_c(t))^2 - c_y(t)(y - y_c(t))^2 - c_z(t)(z - z_c(t))^2], \quad (13)$$

shows that the matrices in the exponential read $\alpha^{(1)}(t) = \delta^{(1)}(t) = 0$, $\beta^{(1)}(t) = 1$ and $\gamma^{(1)}(t) = \frac{2g_i}{m} D(c_x(t), c_y(t), c_z(t))$. A significant simplification arises because $\gamma^{(1)}(t)$ is diagonal: one needs only to compute the exponential of three 2×2 matrices associated with the orthogonal directions O_x, O_y, O_z . The $ABCD$ matrix is simply the tensor product of those:

$$M^{(1)}(t + dt, t, X_0) = \otimes_{j=x,y,z} T \left[\exp \left(\int_{t_0}^t dt' \begin{pmatrix} 0 & 1 \\ \frac{2g_j}{m} c_j(t') & 0 \end{pmatrix} \right) \right] \quad (14)$$

[i] The Hamiltonian $\hat{H}^{(1)}(t)$ and the lensing polynomial $P_l^{(1)}(\mathbf{r}, t)$ depend of course also on X_0 , but we do not mention this dependence explicitly to alleviate the notations.

C. Propagation in a series of infinitesimal lenses.

An infinitesimal expansion of (16) shows that the evolution between t and $t + dt$ is described by the $ABCD$ matrix:

$$M^{(1)}(t, t_0, X_0) \simeq \begin{pmatrix} 1 & dt \\ \frac{2g_i}{m} \mathbf{D}(c_x(t), c_y(t), c_z(t)) & 1 \end{pmatrix} \quad (15)$$

It can be rewritten as a product of two $ABCD$ matrices:

$$M^{(1)}(t + dt, t, X) \simeq \begin{pmatrix} 1 & dt \\ 0 & 1 \end{pmatrix} \begin{pmatrix} 1 & 0 \\ \frac{2g_i}{m} \mathbf{D}(c_x(t), c_y(t), c_z(t)) & 1 \end{pmatrix} \quad (16)$$

If these were 2×2 matrices, in the optical formalism, the first matrix would be associated with the propagation of a ray on the length dt and the second matrix, of the form

$$\begin{pmatrix} 1 & 0 \\ -dt/f & 1 \end{pmatrix} \quad (17)$$

would model a lens of infinitesimal curvature dt/f . One can thus consider, by analogy, that this second 6×6 matrix realizes an atom-optical lens which curvature is the infinitesimal 3×3 matrix $\frac{2g_i}{m} \mathbf{D}(c_x(t), c_y(t), c_z(t)) dt$. Besides, one can exploit the fact that it is a tensor product: if one considers each direction O_x, O_y, O_z separately, the propagation amounts - as in optics - to a product of 2×2 matrices, which makes the analogy with a lens even more transparent. The resulting 6×6 $ABCD$ matrix is simply given by the tensor product of those. Transverse degrees of freedom are, nonetheless, coupled to each other through the lensing potential. It is worth noticing that the focal lengths f_x, f_y, f_z have here the dimension of a time, and are negative if one considers repulsive interactions: the quadratic potential $P_l^{(1)}(\mathbf{r}, \mathbf{p}, t)$ acts as a series of diverging lenses associated with each infinitesimal time slice.

D. Expression of the nonlinear $ABCD$ matrix with the Magnus Expansion.

Because of the time-dependence of the Hamiltonian $\hat{H}^{(1)}(t)$, the time-ordered exponential in (16) cannot, in general, be expressed analytically. Fortunately, a useful expression is provided by the Magnus expansion [34]:

$$M^{(1)}(t, t_0, X_0) = \otimes_{j=x,y,z} \exp \left[\int_{t_0}^t dt_1 N_j(t_1) + \frac{1}{2} \int_0^t dt_1 \int_0^{t_1} dt_2 [N_j(t_1), N_j(t_2)] + \dots \right] \quad \text{with } N_j(t) = \begin{pmatrix} 0 & 1 \\ \frac{2g_i}{m} c_j(t) & 0 \end{pmatrix} \quad (18)$$

This expansion has been successfully applied to solve differential equations in classical and quantum mechanics [35] and later to study spectral line broadening [36], nuclear magnetic resonance [37], multi-photon absorption [38] or strong field effects in saturation spectroscopy [39]. The convergence of this series, discussed in [40], will be admitted here. We express here the nonlinear $ABCD$ matrix to the leading order in the Magnus expansion. A second-order computation can be found in Appendix B.

The first term $\Omega_1(t, t_0)$ of the Magnus expansion can be expressed as

$$\Omega_1(t, t_0) = \int_{t_0}^t dt' N(t') = \begin{pmatrix} 0 & t - t_0 \\ \langle \gamma \rangle (t - t_0) & 0 \end{pmatrix} \quad (19)$$

with the average quadratic diagonal matrix $\langle \gamma \rangle$:

$$\langle \gamma_{jj} \rangle = \frac{g_i}{m(t - t_0)} \int_{t_0}^t \frac{dt'}{w_j^3(t) \prod_{k \neq j} w_k^{1/2}(t)} \quad (20)$$

In our first-order perturbative treatment, the widths $w_j(t)$ follow the free evolution (10). The integrals (20) are given in Eq. (C1) of Appendix C for a cylindrical condensate. Without this symmetry, to our knowledge, the integrals (20) cannot be evaluated analytically, but are nonetheless accessible with efficient numerical methods [i].

[i] In the short expansion limit considered later where $|t - t_0| \ll mw_j(t_0)/\hbar$, the average quantities $\langle \gamma_{jj} \rangle$ can be approximated by the instantaneous value of the quadratic coefficient γ_{jj} at the center of the considered time interval.

The leading-order $ABCD$ matrix reads [i] :

$$M^{(1)}(t, t_0, X_0) \simeq \exp[\Omega_1(t, t_0)] = \begin{pmatrix} \cosh(\langle\gamma\rangle^{1/2}(t-t_0)) & \langle\gamma\rangle^{-1/2} \sinh(\langle\gamma\rangle^{1/2}(t-t_0)) \\ \langle\gamma\rangle^{1/2} \sinh(\langle\gamma\rangle^{1/2}(t-t_0)) & \cosh(\langle\gamma\rangle^{1/2}(t-t_0)) \end{pmatrix} \quad (21)$$

As expected, this main contribution of the Magnus expansion is independent of the ordering of the successive infinitesimal lenses, and can be interpreted as the $ABCD$ matrix of a thick lens with finite curvature. This expression is similar to the paraxial $ABCD$ matrix obtained in [13] to describe the interactions between an atom laser and a condensate of known wave-function.

V. STABILITY ANALYSIS OF A MATTER-WAVE RESONATOR

In this section, we apply the method of the $ABCD$ matrix to discuss the stability of a matter-wave resonator [41]. We consider the propagation of a Gaussian atomic sample in the aberrationless approximation, and we use the leading-order nonlinear $ABCD$ matrix (21) to model the propagation. The evolution of the sample width obtained with this method is compared to the behavior expected from a nonperturbative paraxial approach.

A. Resonator description

The considered matter-wave resonator is based on the levitation of a free-falling two-level atomic sample by periodic vertical Raman light pulses [41]. In the absence of light field, the atomic sample propagates in the Hamiltonian (1). Raman pulses are taken sufficiently far detuned, so that spontaneous emission can be safely neglected [ii] . After adiabatic elimination of the intermediate level, the action of the Raman pulses can be modelled by the effective dipolar Hamiltonian:

$$\hat{H}_{dip}(t) = -\hbar\Omega_{ba}(\mathbf{r}, t) \cos(\omega t - 2\mathbf{k} \cdot \hat{\mathbf{r}} + \phi_0) (|b\rangle\langle a| + |a\rangle\langle b|) \quad (22)$$

The Raman pulses are assumed to be short, resonant and performed successively by two counter-propagating vertical lasers. The sequence is arranged in pairs of successive π pulses with opposite effective wave-vectors. Each pair acts as an atomic mirror, bringing back the atoms in their initial internal state a , and providing them with a net momentum transfer of $\Delta\mathbf{p} \simeq 4\hbar\mathbf{k}$. The atomic motion is sketched on Fig. 1 in the energy-momentum picture.

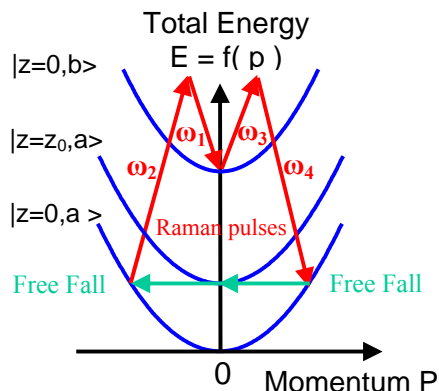


FIG. 1: Evolution of the atomic sample in the energy-momentum picture. The atoms are initially at rest at the altitude z_0 . The total energy includes the kinetic, gravitational and internal energy. As a conservative motion, the free-fall is represented by a leftward horizontal trajectory of the representative point.

[i] For repulsive interactions, all the eigenvalues of the matrix γ are positive, and by convention its square root has also positive eigenvalues.

[ii] As a concrete example, one could consider the ^{87}Rb set on an hyperfine transition to realize this setup, and a detuning of a few GHz in the Raman laser is sufficient to make the effects of spontaneous emission negligible.

If the period T in-between two successive ‘‘Raman mirrors’’ is set to

$$T := T_0 = \frac{mg}{4\hbar k}, \quad (23)$$

the acceleration provided by the Raman pulses compensates on average that of gravity: the cloud levitates and evolves inside a matter-wave resonator [41].

B. Focusing with atomic mirrors.

In the absence of refocusing mechanism, the cloud expands and its diameter quickly exceeds that of the Raman laser beams. In order to keep the sample in levitation, it is thus necessary to operate a transverse confinement. Matter-wave focusing can be obtained, in principle, with laser waves of quadratic intensity profile [42] or of spherical wave-front [41]. These light waves generate a curved Raman mirror, which operates on the widths matrices X, Y of a Gaussian wave-packet through an $ABCD$ matrix of the kind:

$$\begin{pmatrix} A_M & B_M \\ C_M & D_M \end{pmatrix} = \begin{pmatrix} 1 & 0 \\ -1/f_x & 1 \end{pmatrix} \otimes \begin{pmatrix} 1 & 0 \\ -1/f_y & 1 \end{pmatrix} \otimes \begin{pmatrix} 1 & 0 \\ 0 & 1 \end{pmatrix}$$

This expression shows that the Raman mirror acts as a lens in the transverse directions O_x, O_y only; however the absence of focusing in the direction of laser beam propagation O_z is not critical since it does not drive the cloud out of the beam.

The strength of the focusing which can be achieved with such atomic mirrors depends indeed on the desired reflection coefficient. We discuss here qualitatively how this constraint applies for the phase imprinting method used in [42], which rests on the addition of a quadratic phase onto the wave-function. The multiplication of the cloud wave-function with a quadratic phase factor $e^{i\sum_{j=x,y}\alpha_j r_j^2}$ amounts to an $ABCD$ transformation (24) of the Gaussian parameters X, Y [41], with

$$f_{x,y} = \frac{m}{2\hbar\alpha_{x,y}} \quad (24)$$

Such a quadratic light-shift can be obtained to a good approximation with a π pulse of Gaussian intensity profile

$I(\mathbf{r}, t) = I_0(t)e^{-\frac{(x-x_0)^2}{w_{las\ x}^2} + \frac{(y-y_0)^2}{w_{las\ y}^2}}$. The light-shift is proportional to the intensity, so the quadratic coefficients read $\alpha_{x,y} \simeq \phi_0/w_{las\ x,y}^2$ with ϕ_0 the phase imprinted at the condensate center. The phase difference imprinted between the half-width (noted in this paragraph only $w_{cond. x,y}$) and the center of the condensate is on the order of $\Delta\phi \simeq \phi_0 w_{cond. x,y}^2/w_{las. x,y}^2$. In order to obtain an efficient population transfer, one should have $|\Delta\phi| \leq \phi_m \ll \pi$, which gives a lower bound for the focal time $f_{x,y}$:

$$f_{x,y} \geq \frac{m w_{cond. x,y}^2}{2\hbar\phi_m} \quad (25)$$

Atomic clouds of smaller transverse size can thus be focused more efficiently, but are naturally subject to stronger interactions effects for a constant number of atoms. Considering for instance a cylindrical cloud of ^{87}Rb atoms of transverse size $w_{cond. x,y} \simeq 10\ \mu\text{m}$, and a maximum phase difference $\phi_m = 10^{-3}\pi$, one obtains a minimum focusing time: $f \geq 20\text{s}$.

C. Resonator stability analysis.

We now investigate the non-linear $ABCD$ propagation of a cigar-shaped sample in the resonator. As a specific example, we consider a cloud of ^{87}Rb atoms taken in the two internal levels $|a\rangle = |5S_{1/2}, F=1\rangle$ and $|b\rangle = |5S_{1/2}, F=2\rangle$. In-between the Raman mirrors, the whole sample is expected to propagate in the ground state $|a\rangle$. We have used the diffusion length $a \simeq 5,7\ \text{nm}$ [13]. We investigate the evolution of this sample during a thousand bounces and for various mirror focal times. Keeping a significant atomic population inside a matter-wave resonator during such a big number of reflections is challenging, but not impossible in principle given the high population transfer which has been achieved experimentally with Raman pulses [43]. The period between the Raman mirrors $T_0 \simeq 1.5\ \text{ms}$ is much smaller than the time scale $\tau = w_r/\sqrt{\hbar m}$ associated with the free evolution of atomic wave-packets on the order of $100\ \text{ms}$. The

variation of the lensing potential is indeed very small in the time interval separating two successive Raman mirrors. This justifies two approximations. First, one can safely approximate the average quadratic coefficient $\langle \gamma \rangle$ with the instantaneous value $\langle \gamma \rangle \simeq \gamma(w_x(T_0/2), w_y(T_0/2), w_z(T_0/2))$. Second, the second and higher order terms of the Magnus expansion (18) can be neglected, and one may compute the $ABCD$ matrix using the first-order term as in Eq. (21).

Computing the evolution of the transverse and longitudinal sample width is a straightforward numerical task. The results, depicted on Fig. 2, show that the transverse width oscillates with an amplitude and a period which both increase with the mirror focal time. We have considered a sample of $N = 10^5$ atoms and of initial dimensions $w_x = w_y = w_r = 10 \mu m$ and $w_z = 100 \mu m$. This cloud is efficiently confined transversally in the resonator for the considered focal times: its maximum size is $w_r = 25 \mu m$ and $w_r = 60 \mu m$ and for respectively $f = 20 s$ and $f = 100 s$. As expected, the use of Raman mirrors with a stronger curvature allows one to shrink the transverse size of the stabilized cloud. Fig. 3 shows the evolution of the maximum sample transverse size as a function of the mirror focal time. The extended ABCD matrix analysis presented in this paper allows thus to determine efficiently the minimum amount of focusing required to keep the sample within the diameter of the considered Raman lasers. In that respect it can be used to optimize the trade-off, highlighted in the previous paragraph, between strongly focusing or highly reflecting atomic mirrors.

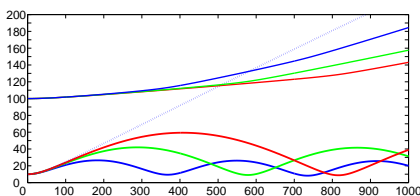


FIG. 2: Evolution of the transverse and longitudinal width of the sample (μm) during the successive bounces in the cavity (numbered from 1 to 1000), for the mirror focal times $f = 20 s$ (blue), $f = 50 s$ (green) and $f = 100 s$ (red). The dashed line represents the evolution of the transverse width in the absence of focusing with the Raman mirrors.

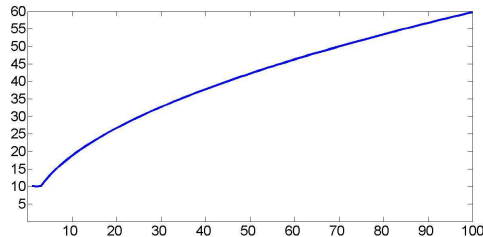


FIG. 3: Maximum sample transverse width (μm) during the evolution in the resonator as a function of the Raman mirror focal time (s). We have considered the first 1000 bounces to determine this maximum.

D. Comparison with the predictions of the nonlinear paraxial equation.

As exposed in Appendix A, the propagation of an atomic beam with a longitudinal momentum much greater than the transverse momenta can be alternatively described by a paraxial wave equation of the form (A2). Furthermore, if the linear density of the atomic beam is uniform, the nonlinear coefficient intervening in this paraxial equation is a constant. As in nonlinear optics [44] and in 2D condensates [45], this equation induces a universal behavior in paraxial atomic beams [46]: the transverse width oscillates with a frequency independent from the strength of the interaction. The width oscillations, depicted on Fig. 2, indeed allow one to confront the results of our method, which uses a non-paraxial wave equation treated in the aberrationless approximation, to the predictions of the full nonlinear paraxial equation with a uniform nonlinear coefficient. We stress that this second approach leaves the nonlinear term as such and does not assume that the Gaussian shape of the atomic beam is preserved. In this sense it is more exact than the radius of curvature method used in Appendix A. It is also approximate, since the atomic beam is neither

paraxial nor of uniform linear density. Nevertheless, it is remarkable that both treatments agree very well on the oscillation period of the width.

To apply the paraxial description, one models the action of the successive mirrors on the transverse wave-function with an average potential. The lens operated by each Raman mirror, of focal time $f_x = f_y = f$, imprints a phase factor of $e^{i\frac{m}{2\hbar f}r^2}$ [see Eq. (24)]. The series of lenses, separated by the duration T_0 , thus mimics the following effective quadratic potential:

$$V_{\perp, lens} = \frac{m}{2\hbar^2 T_0 f} r^2 \quad (26)$$

Adding the nonlinear contribution approximated by a contact term of constant strength [i] $V_{\perp, int}(\mathbf{r}) = \beta|\psi_{\perp}(\mathbf{r})|^2\psi_{\perp}(\mathbf{r})$ to Eq. (A1), one obtains a 2D nonlinear Schrödinger equation (NLSE):

$$i\hbar\partial_{\zeta}\psi_{\perp}(x, y, \zeta) = \left[-\frac{\hbar^2}{2m}(\partial_x^2 + \partial_y^2) + \beta|\psi_{\perp}(x, y, \zeta)|^2 + \frac{m}{2\hbar^2 T_0 f} r^2 \right] \psi_{\perp}(x, y, \zeta), \quad (27)$$

ζ is a parameter defined in Eq. (A1) equivalent to the propagation time. Setting $K = \frac{m}{\hbar}$, one can recast this equation in the same form as the propagation of a light wave in a quadratic graded index medium [44]:

$$2iK\partial_{\zeta}\psi_{\perp}(x, y, \zeta) = \left[-\partial_T^2 + \gamma|\psi_{\perp}(x, y, \zeta)|^2 + K^2 \left(\frac{1}{fT_0} \right) \right] \psi_{\perp}(x, y, \zeta), \quad (28)$$

with a constant γ which we do not need to explicit. As shown in [44, 46], such equation yields transverse oscillations of universal frequency:

$$\omega_{par} = \frac{2}{\sqrt{fT_0}}$$

The results obtained from the perturbative ABCD approach are confronted with this prediction on Fig. 4. The agreement improves as the mirror focal time increases, and it is in fact already good (4%) for a focal time of $f = 3s$ and attains 0.7% for a focal time of $f = 50s$. As discussed above, focal times shorter than $f = 20s$ seem incompatible with the reflection coefficient desired for the atomic mirrors. The disagreement observed below $f \leq 3s$ may be attributed to a failure of the paraxial approximation.

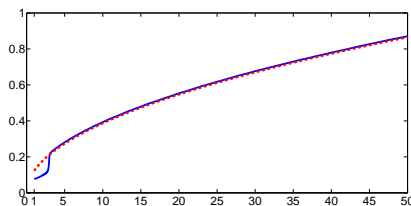


FIG. 4: Period of the transverse width oscillations (s) in the matter-wave resonator as a function of the Raman mirror focal time (s). The full and the dashed line give the oscillation periods obtained respectively through the perturbative ABCD approach and through the nonlinear paraxial wave equation.

VI. CONCLUSION

This paper exposed a treatment of the non-linear Schrödinger equation involving theoretical tools from optics and atom-optics. The *ABCD* propagation method for matter waves has been extended beyond the linear regime thanks to a perturbative analysis relying on an atom-optical aberrationless approximation. It has been applied to discuss

[i] The coefficient β is indeed a constant only if the linear atomic density is uniform, which is not the case here.

the stabilization of a matter-wave resonator thanks to curved atomic mirrors. This method reproduces to a good level of accuracy the universal oscillations expected from the nonlinear paraxial equation for matter waves [46], which makes it a promising tool to model future nonlinear atom optics experiments. We also highlighted another optical method, involving more stringent assumptions - paraxial propagation, cylindrical symmetry and constant longitudinal velocity - and also relying on the aberrationless approximation. Both approaches are relevant to study interaction effects on the stability of atomic sensors resting on Bloch oscillations [47] or on the sample propagation in coherent interferometers [48]. An interesting continuation of this work would be to develop a nonlinear ABCD matrix analysis beyond the aberrationless approximation.

ACKNOWLEDGEMENTS

The authors acknowledge enlightening discussions with Yann Le Coq on the nonlinear paraxial equation for matter waves. François Impens thanks Nicim Zagury and Luiz Davidovich for their hospitality. This work was supported by DGA (Contract No 0860003) and by CNRS. Our research teams in SYRTE and Laboratoire de Physique des Lasers are members of IFRAF (www.ifraf.org).

APPENDIX A: THE METHOD OF THE NON-LINEAR RADIUS OF CURVATURE.

This method addresses the paraxial propagation of a monochromatic and cylindrical matter-wave beam. It relies on the introduction of an effective complex radius of curvature [18, 21], which evolution is especially simple, even for a self-interacting beam. It has been applied successfully by Bélanger and Paré [19] to describe self focusing phenomena of cylindrical optical beams propagating in the paraxial approximation, and it works equally well for matter waves propagating in the same regime. This is typically the case for an atom laser beam falling into the gravity field, for which the transverse momentum components become negligible compared to the vertical momentum after sufficient time [13].

We consider a monoenergetic wave-packet propagating in the paraxial regime, and evolving in the sum of a longitudinal potential $V_{//}(z)$ and a transverse one $V_{\perp}(x, y, z)$, which may also vary slowly with the longitudinal coordinate z . This section begins with a brief reminder on the paraxial equation for matter waves [28], and on its spherical-wave solutions in the linear case [18]. It is remarkable that such solutions can be extended to the nonlinear propagation [18], at the cost of certain approximations, and thanks to the introduction of a generalized radius of curvature depending on the coupling strength. Our treatment of the nonlinear matter wave propagation follows step by step the approach of Bélanger and Paré for optical waves [19].

1. The Paraxial Equation for Matter Waves.

Our derivation of the nonlinear paraxial wave-equation follows the treatment done in [28]. The wave-function is factorized into a transverse and longitudinal component:

$$\psi(x, y, z) = \psi_{\perp}(x, y, z) \psi_{//}(z)$$

The longitudinal component obeys a 1D time-independent Schrödinger equation,

$$-\frac{\hbar^2}{2m} \frac{\partial^2 \psi_{//}}{\partial z^2} + V_{//} \psi_{//} = E \psi_{//},$$

which can be solved with the WKB method:

$$\psi_{//}(z) = \sqrt{\frac{m\mathcal{F}}{p(z)}} \exp\left[\frac{i}{\hbar} \int_{z_0}^z du p(u)\right].$$

$\mathcal{F} = \int d^2\mathbf{r}_{\perp} \frac{p(z)}{m} |\psi(\mathbf{r}_{\perp}, z)|^2$ is the atomic flux evaluated through any infinite transverse plane, the transverse wave-function ψ_{\perp} being normalized to unity $\int d^2\mathbf{r}_{\perp} |\psi_{\perp}(\mathbf{r}_{\perp}, z)|^2 = 1$. $p(z) = \sqrt{2m(E - V_{//}(z))}$ is the classical momentum along z , and z_0 is the associated classical turning point verifying $p(z_0) = 0$. The transverse wave-function ψ_{\perp} , assumed to depend slowly enough on the coordinate z to make its second derivative negligible, verifies the equation:

$$\left[i\hbar \frac{p(z)}{m} \partial_z + \frac{\hbar^2}{2m} (\partial_x^2 + \partial_y^2) - V_{\perp}(x, y, z) \right] \psi_{\perp}(x, y, z) = 0,$$

This equation can be simplified with a variable change in which the longitudinal coordinate z is replaced by the parameter ζ :

$$\zeta(z) = \int_{z_0}^z dz \frac{m}{p(z)} \quad (\text{A1})$$

which corresponds to the time needed classically to propagate from the turning point z_0 to the coordinate z [i]. The wave equation becomes

$$\left[i\hbar\partial_\zeta + \frac{\hbar^2}{2m}(\partial_x^2 + \partial_y^2) - V_\perp(x, y, \zeta) \right] \psi_\perp(x, y, \zeta) = 0, \quad (\text{A2})$$

We assume from now on that the transverse potential $V_\perp(x, y, z)$ has a cylindrical symmetry. If one sets $K = m/\hbar$ and $V_\perp(x, y, \zeta) = \frac{\hbar^2}{2}K_2(\zeta)r^2$ with $r^2 = x^2 + y^2$, Eq. (A2) has the same form as the paraxial equation for the electric field used in [19]:

$$[\partial_T^2 + 2iK\partial_\zeta - KK_2(\zeta)r^2] \psi_\perp(x, y, \zeta) = 0, \quad (\text{A3})$$

It is worth noticing that, as a consequence of our variable change, the derivative with respect to the longitudinal coordinate z has been replaced by a time derivative with respect to ζ .

2. Spherical Wave solutions to the linear equation.

One looks for solutions of Eq. (A3) of the kind:

$$\psi_\perp(x, y, \zeta) = A(\zeta) \exp \left[i \frac{K}{2q(\zeta)} r^2 \right] \quad (\text{A4})$$

with again $K = m/\hbar$. Such function is a solution if and only if the parameter $q(\zeta)$ - called complex radius of curvature, and homogenous to a time for matter waves - satisfies the following equation:

$$\frac{q' - 1}{q^2} - \frac{K_2(\zeta)}{K} = 0 \quad (\text{A5})$$

and if the amplitude $A(\zeta)$ verifies:

$$\frac{A'}{A} + \frac{1}{q} = 0 \quad (\text{A6})$$

The prime stands for the derivative with respect to ζ . In the absence of the transverse potential, i.e. $V_\perp(x, y, \zeta) = 0$, an obvious evolution is obtained with $q(\zeta) = \zeta$.

These equations imply a relation between the amplitude and width of the wave-function. We adopt the usual decomposition for the complex radius of curvature along its imaginary and complex part:

$$\frac{1}{q} = \frac{1}{R} + \frac{2i}{Kw^2}$$

Assuming that $K_2(\zeta)$ is real, and combining the imaginary part of Eq. (A5) with the real part of Eq. (A6), one obtains:

$$|A(\zeta)|^2 = |A_0|^2 \frac{w_0^2}{w^2(\zeta)}$$

This relation reflects the conservation of the atomic flux \mathcal{F} along the propagation. With our choice of normalization, the parameter $|A|^2$ is given by:

$$|A|^2 = \frac{2}{\pi w^2} \quad (\text{A7})$$

[i] Indeed, this parameter appear as proportional to the proper time experienced by the atom on the classical trajectory determined by $p(z)$ [49].

3. Spherical Wave solutions to the nonlinear equation.

With several approximations, it is possible to find similar solutions in the interacting case. Atomic interactions are described by the mean-field potential

$$V_i(x, y, \zeta) = g_i^0 |\psi_{//}(z)|^2 |\psi_{\perp}(x, y, \zeta)|^2 \quad \text{with} \quad g_i^0 = \frac{4\pi\hbar^2 a_s}{m}$$

which intervenes in the time-independent equation verified by ψ . a_s denotes the atomic scattering length. This induces the following transverse potential

$$V_{\perp}(x, y, \zeta) = g_i^0 |\psi_{//}(\zeta)|^2 (|\psi_{\perp}(x, y, \zeta)|^2 - |\psi_{\perp}(0, 0, \zeta)|^2)$$

in the paraxial equation verified by ψ_{\perp} . In the considered example, this potential receives no other contribution. The subsequent analysis requires three important approximations. First, it uses the ‘‘aberrationless approximation’’, which assumes that the wave-function follows the Gaussian profile (A4) in spite of the non-linearity. Second, it assumes that the transverse mean-field potential is well-described by a second order expansion,

$$V_{\perp}(x, y, \zeta) \simeq -g_i^0 |\psi_{//}(\zeta)|^2 \frac{|A(\zeta)|^2}{w^2(\zeta)} r^2 \quad (\text{A8})$$

The term $G(\zeta) = g_i^0 |\psi_{//}(\zeta)|^2$ can be seen as the atom-optical equivalent of a third-order non-linear permittivity. Third, it neglects the dependence on $G(\zeta)$ towards the altitude, which is a valid approach if the linear density $n_{1D}(z) = m\mathcal{F}/p(z)$ is uniform, which we assume from now on [i]. Eq. (A8) and the normalization of ψ_{\perp} [Eq. (A7)] give readily:

$$\frac{K_2(\zeta)}{K} = \frac{-2g_i^0 \mathcal{F}}{\pi p_{0//} w^4(\zeta)}$$

Eq. (A5) can then be recast as:

$$\frac{q' - 1}{q^2} + 2n_{1D}a_s \left(\frac{4}{K^2 w^4(\zeta)} \right) = 0$$

The last equation may be split into its real and imaginary part along:

$$\left(\frac{1}{R} \right)' + \frac{1}{R^2} - \sigma \left(\frac{2}{Kw^2} \right)^2 = 0 \quad (\text{A9})$$

and

$$\left(\frac{1}{Kw^2} \right)' + 2 \left(\frac{1}{R} \right) \left(\frac{2}{Kw^2} \right) = 0 \quad (\text{A10})$$

where we have introduced the dimensionless parameter $\sigma = 1 + 2n_{1D}a_s$. This system can be uncoupled thanks to the following trick: Eq. (A10) is multiplied by $i\sqrt{\sigma}$ and added to Eq. (A9). One obtains:

$$\left(\frac{1}{R} \right)' + i\sqrt{\sigma} \left(\frac{2}{Kw^2} \right)' + \frac{1}{R^2} + \frac{2i\sqrt{\sigma}}{R} \left(\frac{2}{Kw^2} \right) - \sigma \left(\frac{2}{Kw^2} \right)^2 = 0 \quad (\text{A11})$$

This equation can be simply interpreted as

$$q'_{NL} - 1 = 0 \quad (\text{A12})$$

with the generalized complex radius of curvature:

$$q_{NL} = \frac{1}{R} + \frac{2\sqrt{\sigma}i}{Kw^2} \quad (\text{A13})$$

[i] A similar approximation on the constant width of the longitudinal wave-packet is indeed implicit in the treatment of Bélanger and Paré [19], since it is necessary to obtain a nonlinear paraxial wave-equation which involves only the transverse wave-function.

Its very simple evolution

$$q_{NL}(\zeta) = q_{NL}(\zeta_0) + \zeta - \zeta_0 \quad (\text{A14})$$

gives readily the real radius of curvature $R(\zeta)$ and the width $w(\zeta)$ as a function of the time ζ . These quantities can be expressed as a function of the altitude z thanks to Eq. (A1). In the specific case of constant atomic flux \mathcal{F} and constant average longitudinal momentum $p(z) = \sqrt{2m(E - V_{//}(z))} \simeq p_{0//}$, this correspondence is especially simple: the parameter ζ is given $\zeta = m(z - z_0)/p_{0//}$, and Eq. (A14) can be recast as:

$$q_{NL}(z) = q_{NL}(z_0) + \frac{m(z - z_0)}{p_{0//}} \quad (\text{A15})$$

One thus has, as in the linear case, a simple spherical-wave solution (A4). Indeed, this method allows one to approximate very efficiently the nonlinear propagation of a wave-function of initial Gaussian profile. As in optics, this treatment can be applied to discuss the self focusing for matter waves. It is, however, important to keep in mind its validity domain and the several hypothesis required - constant longitudinal velocity, cylindrical symmetry and paraxial propagation -.

APPENDIX B: NONLINEAR ABCD MATRIX EVALUATED TO SECOND-ORDER.

In this Appendix, we discuss the nonlinear corrections to the $ABCD$ matrix associated with the second-order of the Magnus expansion $\Omega_2(t, t_0)$, which reads:

$$\Omega_2(t, t_0) = \frac{1}{2} \int_{t_0}^t dt_1 \int_{t_0}^{t_1} dt_2 [N(t_1), N(t_2)] = \begin{pmatrix} S(t, t_0) & 0 \\ 0 & -S(t, t_0) \end{pmatrix} \quad S(t) = \int_{t_0}^t dt_1 \int_{t_0}^{t_1} dt_2 (\gamma(t_1) - \gamma(t_2)) \quad (\text{B1})$$

This term, arising from the non-commutativity between the Hamiltonians taken at different times, naturally depends on the ordering chosen for the successive lenses. Because of the cloud expansion, lenses are ordered from the most divergent to the less divergent. To discuss the effect of this second-order contribution on the wave-function, it is useful to compute the exponential:

$$\exp[\Omega^{(2)}(t, t_0)] = \begin{pmatrix} e^{S(t, t_0)} & 0 \\ 0 & e^{-S(t, t_0)} \end{pmatrix} \quad (\text{B2})$$

The action of such matrix onto the position-momentum width vector (X, Y) , defined in Sec. III A, would operate a squeezing between position and momentum. This squeezing is indeed a consequence of our aberrationless approximation, in which the propagation leaves the phase-space volume invariant: the expansion of the cloud size must be, in our treatment, compensated by a reduced momentum dispersion. One finds consistently that the diagonal matrix elements $S_{xx,yy,zz}(t)$, involved in (B2), are positive, which results from the decrease of the matrix elements $\gamma_{xx,yy,zz}(t)$ with time.

The $ABCD$ matrix obtained from the two first terms of the Magnus expansion reads:

$$M^{(1)}(t, t_0, X_0) \simeq \otimes_{i=x,y,z} \begin{pmatrix} \cosh K_i(t, t_0) + S_{ii}(t, t_0) \frac{\sinh K_i(t, t_0)}{K_i(t, t_0)} & \langle \gamma \rangle^{-1/2} \frac{\sinh K_i(t, t_0)}{K_i(t, t_0)} \\ \langle \gamma \rangle^{1/2} \frac{\sinh K_i(t, t_0)}{K_i(t, t_0)} & \cosh K_i(t, t_0) - S_{ii}(t, t_0) \frac{\sinh K_i(t, t_0)}{K_i(t, t_0)} \end{pmatrix} \quad (\text{B3})$$

We have introduced the functions $K_i(t, t_0) = \sqrt{S_{ii}^2(t, t_0) + \langle \gamma_{ii} \rangle^2 (t - t_0)^2}$. Again, an analytic expression of $\langle \gamma_{ii} \rangle$ and $S_{ii}(t, t_0)$ can be found for cigar-shaped condensates in Eq. (C1) and Eq. (C2) of Appendix C. Higher-order contributions to the $ABCD$ matrix (18) can be computed along similar guidelines, but they involve various integrations which need to be performed numerically.

APPENDIX C: ABCD MATRIX ELEMENTS FOR THE CIGAR-SHAPED CONDENSATE

We evaluate in this appendix various primitives necessary to explicit the non-linear $ABCD$ matrix to first and second order in the Magnus expansion given in Eq. (21) and Eq. (B3). We consider a cigar-shaped cylindrical condensate with a long vertical extension: $w_x = w_y = w_r \ll w_z$. We remind the linear evolution of the width given by Eq. (10) i.e. $w_{r,z}(t) = \sqrt{w_{r,z}^2 + \Delta v_{r,z}^2 (t - t_0)^2}$. We shall use the short-hand notation $w_{r,z} = w_{r,z}(t_0)$ and $\Delta v_{r,z} = \hbar/(mw_{r,z}(t_0))$.

1. Average quadratic coefficient.

We seek to evaluate:

$$\gamma_{rr}(t) = \frac{g_i}{(2\pi)^{3/2} m w_z(t) w_r(t)^4} \quad \gamma_{zz}(t) = \frac{g_i}{(2\pi)^{3/2} m w_z(t)^3 w_r(t)^2}$$

We note $\gamma_0 = g_i / [(2\pi)^{3/2} m]$ and $\Lambda(t)$ the function:

$$\Lambda(t) = \frac{\sqrt{\Delta v_r^2 w_z^2 - w_r^2 \Delta v_z^2} (t - t_0)}{w_r w_z(t)}$$

The elements of the matrix $\bar{\gamma}$ are readily obtained:

$$\begin{aligned} \bar{\gamma}_{rr} &= \gamma_0 \left[\frac{\Delta v_r^2 w_z(t)}{2w_r^2 (\Delta v_r^2 w_z^2 - w_r^2 \Delta v_z^2) w_r^2(t)} + \frac{(\Delta v_r^2 w_z^2 - 2w_r^2 \Delta v_z^2) \text{Arctan } \Lambda(t)}{2w_r^3 (\Delta v_r^2 w_z^2 - w_r^2 \Delta v_z^2)^{3/2} (t - t_0)} \right] \\ \bar{\gamma}_{zz} &= \gamma_0 \left[\frac{\Delta v_z^2}{w_z^2 (\Delta v_z^2 w_r^2 - \Delta v_r^2 w_z^2) w_z(t)} + \frac{\Delta v_r^2 \text{Arctan } \Lambda(t)}{w_r (\Delta v_r^2 w_z^2 - w_r^2 \Delta v_z^2)^{3/2} (t - t_0)} \right] \end{aligned} \quad (\text{C1})$$

2. Second-order Magnus term.

We evaluate here the matrix $S(t)$. Its computation involves tedious algebra:

$$\begin{aligned} S_{rr}(t, t_0) &= -\frac{\gamma_0}{4w_r^3 \Delta v_r (\Delta v_r^2 w_z^2 - w_r^2 \Delta v_z^2)^{3/2} w_r^2(t)} \times \left[\Delta v_r (t - t_0) (2w_r^2 \Delta v_z^2 - \Delta v_r^2 w_z^2) w_r^2(t) \text{Arctan } \Lambda(t) \right. \\ &\quad - w_r \Delta v_r \sqrt{\Delta v_r^2 w_z^2 - w_r^2 \Delta v_z^2} (2w_r^2 + \Delta v_r^2 (t - t_0)^2) w_r(t) - 2w_r^3 \Delta v_z^2 w_r^2(t) \log \left(\frac{w_r(t)}{w_r} \right) \\ &\quad \left. + w_r^3 \Delta v_z^2 w_r^2(t) \log \left(\frac{w_r^2 \Delta v_z^2 - 2\Delta v_r^2 w_z^2 + 2\Delta v_r \sqrt{\Delta v_r^2 w_z^2 - w_r^2 \Delta v_z^2} w_z(t) - \Delta v_r^2 \Delta v_z^2 (t - t_0)^2}{w_r^2 \Delta v_z^2 - 2\Delta v_r^2 w_z^2 + 2\Delta v_r \sqrt{\Delta v_r^2 w_z^2 - w_r^2 \Delta v_z^2} w_z} \right) \right] \\ S_{zz}(t, t_0) &= \frac{\gamma_0 w_z(t)}{w_z^2 (w_r^2 \Delta v_z^2 - \Delta v_r^2 w_z^2)} + \frac{\gamma_0 \Delta v_r^2 (t - t_0) \text{Arctan } \Lambda(t)}{2w_r (\Delta v_r^2 w_z^2 - w_r^2 \Delta v_z^2)^{3/2}} + \frac{\gamma_0 \Delta v_z^2 (t - t_0)^2}{2w_z^2 (\Delta v_r^2 w_z^2 - w_r^2 \Delta v_z^2) w_z(t)} \\ &\quad + \frac{\gamma_0 \Delta v_r \text{Arctanh} \left(\frac{\Delta v_r (t - t_0)}{w_r \Lambda(t)} \right)}{(\Delta v_r^2 w_z^2 - w_r^2 \Delta v_z^2)^{3/2}} \end{aligned} \quad (\text{C2})$$

-
- [1] C. J. Bordé, in *Fundamental Systems in Quantum Optics* (1990), Les Houches Lectures, Session LIII.
[2] G. Lenz, P. Meystre, and E. M. Wright, *Phys. Rev. Lett.* **71**, 3271 (1993).
[3] W. Zhang and D. F. Walls, *Phys. Rev. A* **49**, 3799 (1994).
[4] E. W. Hagley, L. Deng, M. Kozuma, M. Trippenbach, Y. B. Band, M. Edwards, M. Doery, P. S. Julienne, K. Helmerson, S. L. Rolston, et al., *Phys. Rev. Lett.* **83**, 3112 (1999).
[5] S. Burger, K. Bongs, S. Dettmer, W. Ertmer, K. Sengstock, A. Sanpera, G. V. Shlyapnikov, and M. Lewenstein, *Phys. Rev. Lett.* **83**, 5198 (1999).
[6] J. Denschlag, J. Simsarian, D. Feder, C. Clark, L. Collins, J. Cubizolles, L. Deng, E. Hagley, K. Helmerson, W. Reinhardt, et al., *Science* **287**, 97 (2000).
[7] L. Khaykovich, F. Schreck, G. Ferrari, T. Bourdel, J. Cubizolles, L. D. Carr, Y. Castin, and C. Salomon, *Science* **17**, 1290 (2002).
[8] K. E. Strecker, G. B. Partridge, A. G. Truscott, and R. G. Hulet, *Nature* **417** (2002).
[9] M. R. Matthews, B. P. Anderson, P. C. Haljan, D. S. Hall, C. E. Wieman, and E. A. Cornell, *Phys. Rev. Lett.* **83**, 2498 (1999).
[10] K. W. Madison, F. Chevy, W. Wohlleben, and J. Dalibard, *Phys. Rev. Lett.* **84**, 806 (2000).
[11] S. Inouye, A. P. Chikkatur, D. M. Stamper-Kurn, J. Stenger, D. E. Pritchard, and W. Ketterle, *Science* **285**, 571 (1999).
[12] S. Inouye, T. Pfau, S. Gupta, A. P. Chikkatur, A. Goerlitz, D. E. Pritchard, and W. Ketterle, *Nature* **402**, 641 (December 1999).

- [13] Y. LeCoq, J. H. Thywissen, S. A. Rangwala, F. Gerbier, S. Richard, G. Delannoy, P. Bouyer, and A. Aspect, *Phys. Rev. Lett.* **87**, 170403 (2001).
- [14] T. Busch, M. Köhl, T. Esslinger, and K. Mølmer, *Phys. Rev. A* **65**, 043615 (2002).
- [15] Y. Castin and R. Dum, *Phys. Rev. Lett.* **77**, 5315 (1996).
- [16] H. Michinel, *Pure Appl. Opt.* 701-708 **4**, 701 (1995).
- [17] V. M. Perez-Garcia, P. J. Torres, and G. Montesinos, *SIAM J. Appl. Math.* **67**, 990 (2007).
- [18] A. Yariv and P. Yeh, *Opt. Commun.* **27**, 295 (1978).
- [19] P.-A. Bélanger and C. P. é, *Applied Optics* **22**, 1293 (1983).
- [20] C. J. Bordé, *Metrologia* **39**, 435 (2001).
- [21] H. Kogelnik, *Bell System Technical Journal* **44**, 455 (1965).
- [22] B. K. Garside, *IEEE Journal of Quantum Electronics* **4**, 940 (1968).
- [23] A. Le Floch, R. Le Naour, J. M. Lenormand, and J. P. Taché, *Phys. Rev. Lett.* **45**, 544 (1980).
- [24] F. Bretenaker, A. Le Floch, and J. P. Taché, *Phys. Rev. A* **41**, 3792 (1990).
- [25] F. Bretenaker and A. Le Floch, *Phys. Rev. A* **42**, 5561 (1990).
- [26] V. Magni, G. Cerullo, and S. D. Silvestri, *Opt. Commun.* **96**, 348 (1993).
- [27] J.-F. Riou, W. Guerin, Y. LeCoq, M. Fauquembergue, V. Josse, P. Bouyer, and A. Aspect, *Phys. Rev. Lett.* **96**, 070404 (2006).
- [28] J.-F. Riou, Y. LeCoq, F. Impens, W. Guerin, C. J. Bordé, A. Aspect, and P. Bouyer, *Phys. Rev. A* **77**, 033630 (2008).
- [29] M. Peskin and D. Schroeder, *An Introduction to Quantum Field Theory* (Addison-Wesley Advanced Book Program, 1995).
- [30] C. J. Bordé, *C. R. Acad. Sci. Paris* **4**, 509 (2001).
- [31] C. J. Bordé, J.-C. Houard, and A. Karasiewicz, *Gyros, Clocks and Interferometers: Testing relativistic gravity in space Springer-Verlag* (2000), pp. 403–438.
- [32] C. J. Bordé, *General Relativity and Gravitation* **36**, 475 (2004).
- [33] F. Impens, *Phys. Rev. A* **77**, 013619 (2008).
- [34] W. Magnus, *Comm. Pure Appl. Math* **7**, 649 (1954).
- [35] R. A. Marcus, *J. Chem. Phys.* **52**, 4803 (1970).
- [36] W. A. Cady, *J. Chem. Phys.* **60**, 3318 (1974).
- [37] J. S. Waugh, *J. Magn. Reson.* **50**, 30 (1982).
- [38] I. Schek, J. Jortner, and M. L. Sage, *Chem. Phys.* **59**, 11 (1981).
- [39] J. Ishikawa, F. Riehle, J. Helmcke, and C. J. Bordé, *Phys. Rev. A* **49**, 4794 (1994).
- [40] F. M. Fernández, *Phys. Rev. A* **41**, 2311 (1990).
- [41] F. Impens, P. Bouyer, and C. J. Bordé, *Appl. Phys. B* **84**, 603 (2006).
- [42] G. Whyte, P. Öhberg, and J. Courtial, *Phys. Rev. A* **69**, 053610 (2004).
- [43] M. Weitz, B. C. Young, and S. Chu, *Phys. Rev. Lett.* **73**, 2563 (1994).
- [44] C. Pare and P. Belanger, *Optical and Quantum Electronics* **24**, S1051 (1992).
- [45] L. P. Pitaevskii and A. Rosch, *Phys. Rev. A* **55**, R853 (1997).
- [46] F. Impens, to be published (2008).
- [47] P. Cladé, S. Guellati-Khelifa, C. Schwob, F. Nez, L. Julien, and F. Biraben, *Europhys. Lett.* **71**, 730 (2005).
- [48] Y. L. Coq, J. Retter, S. Richard, A. Aspect, and P. Bouyer, *Appl. Phys. B: Laser and Optics* **84**, 627 (2006).
- [49] C. J. Bordé, in *Proc. of the Enrico Fermi International School of Physics “Atom Optics and Space Physics”*, edited by E. Arimondo, W. Ertmer, and W. Schleich (IOS Press, 2007), and to be published.